JOURNAL OF MATERIALS SCIENCE 27 (1992) 4741–4745

Effect of addition of the $CuO–Fe_2O_3$ system on the electromagnetic wave absorbing properties of sintered ferrite

K. Y. KIM, W. S. KIM, Y. D. JU, H. J. JUNG
Division of Ceramics, Korea Institute of Science and Technology, PO Box 131, Cheongryang, Seoul, Korea

The effects of the addition of the $CuO–Fe_2O_3$ system as a liquid former on the microstructure and electromagnetic wave absorbing property of sintered Ni–Zn ferrite were investigated. The $CuO–Fe_2O_3$ system, a spinel ferrite, has its own magnetic property, which enables it to be used as an electromagnetic wave absorber. The $CuO–Fe_2O_3$ system was preferentially located at the grain boundary in the matrix of an Ni–Zn ferrite. This resulted in an increase in the total loss and a decrease in matching thickness. The centre frequency shift is presumed to occur because Ni–Zn ferrite with $CuO–Fe_2O_3$ behaves like a mixture of two ferrites with loss characteristics at the different frequency ranges.

1. Introduction

As infomation-oriented modern society develops and diversifies with rapid advancement of communication technology, "wave pollution" problems are drawing extensive public concern. The most common examples of such pollution are the ghost phenomenon on TV sets and malfuction of electronic equipment, caused by interference of unwanted electromagnetic waves of external sources. As a solution, various attempts have been directed towards improving wave transmitting and receiving systems. Another approach that has proved most effective is to absorb unnecessary waves using wave-absorbing materials. Such materials are required to have large electromagnetic loss in the frequency range of interest, and proper modification of electromagnetic properties at the particular frequencies [1, 2].

The most widely used material as an electromagnetic wave absorber is ferrite, which has a low frequency range to be used, due to its resonance characteristics. Various attempts to overcome such limitations have been made [3, 4]. For ferrites, liquid-forming agents used as sintering aids are generally non-magnetic dielectrics, which diminish the loss property of magnets by forming electrically insulating films on the particle surfaces [5]. This detrimental effect can be overcome by the use of sintering aids that possess magnetic loss property and enhance the conductivity at particle surface boundaries.

TABLE I Experimental compositions of the $CuO–Fe_2O_3$ system (mol %)

	A	B	C	D	E
CuO	40	45	50	55	60
Fe_2O_3	60	55	50	45	40

In this work, the effect of the addition of the $CuO–Fe_2O_3$ system, a ferrite with a melting temperature of $\sim 1150\,°C$, as a liquid former, on the microstructure and electromagnetic wave-absorbing properties of sintered Ni–Zn ferrite, was investigated.

2. Specimen fabrication and measurements

The compositions of the $CuO–Fe_2O_3$ system employed in the present experiment are listed in Table I. These compositions were selected because they have a liquidus temperature of 1150–1200 °C as shown in the $CuO–Fe_2O_3$ phase diagram (Fig. 1).

The constituent materials were weighed, ball-milled for 24 h and then dried in an oven at 80 °C. The mixture was pressed into coaxial forms (outer diameter of 7 mm, inner diameter of 3 mm) and the $CuO–Fe_2O_3$ systems were sintered in air at 1150 °C for 1 h.

Complex permittivity, permeability and wave loss were measured by coaxial-type measuring equipment and a network analyser as shown in Fig. 2, to determine the effects of the CuO/Fe_2O_3 ratio on these parameters [6].

The samples were prepared by adding 1, 3 and 5 wt % $CuO–Fe_2O_3$ system to Ni–Zn ferrite ($Ni_{0.6}Zn_{0.4}Fe_2O_4$) pre-calcined at 900 °C, followed by sintering the mixture at 1200 °C for 1 h. The measured results for these samples were compared with those for reference specimens made of monolithic Ni–Zn ferrite without addition of $CuO–Fe_2O_3$.

3. Results and discussion

3.1. Magnetic properties of the $CuO–Fe_2O_3$ system

Fig. 3 illustrates the relationship between the real part of permeability and frequency for $CuO–Fe_2O_3$

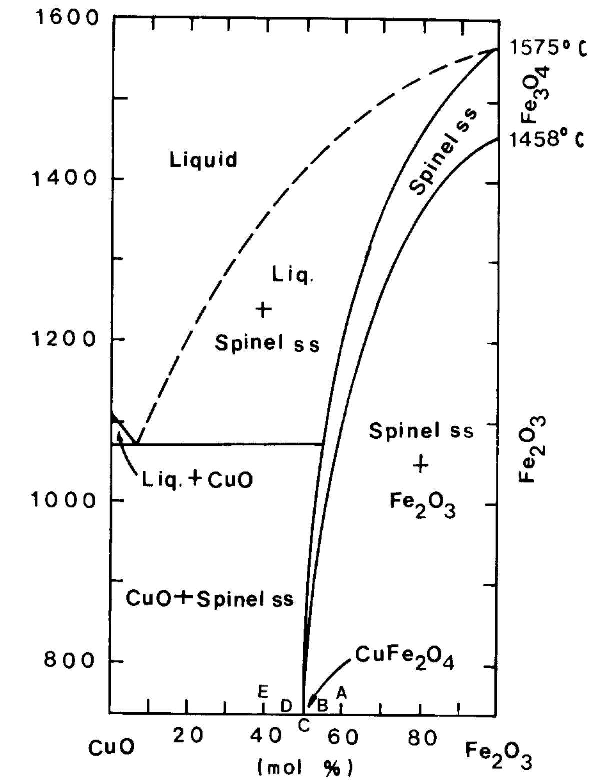

Figure 1 Phase diagram and experimental compositions of the $CuO-Fe_2O_3$ systems.

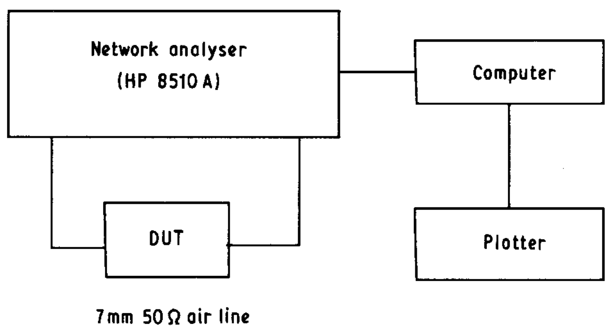

Figure 2 Arrangement of the measuring system.

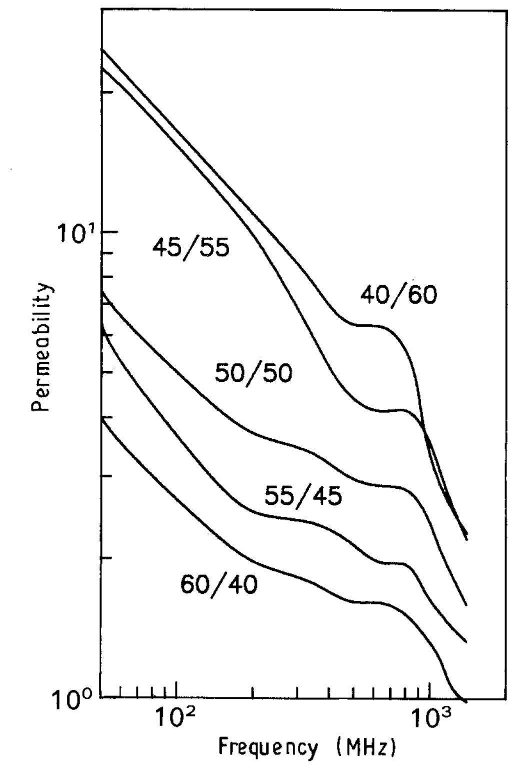

Figure 3 Real part of permeability for $CuO-Fe_2O_3$ systems (mol %) versus frequency.

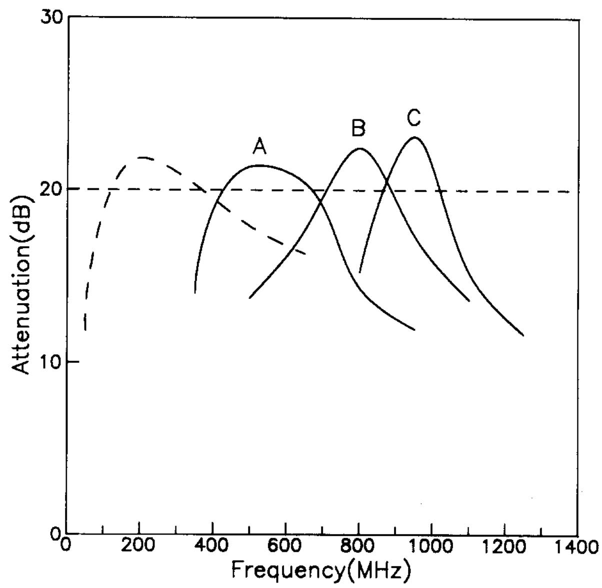

Figure 4 Attenuation behaviour of monolithic Ni–Zn ferrite with compositions A, B and C of $CuO-Fe_2O_3$ systems.

samples. Permeability generally decreased with increasing amount of CuO. This observation agrees with the fact that the theoretical magnetic moment, μ_B, decreases from 4 for monolithic Fe_3O_4 to 1 for stoichiometric composition $CuFe_2O_4$, as the amount of CuO increases.

The resonance frequency decreases as the initial permeability increases [7]. Thus the effective frequency range, where over 20 dB loss occurs, shifted to higher frequency as the amount of CuO increased (Fig. 4).

3.2. Effects of $CuO-Fe_2O_3$ addition on properties of sintered ferrites

$CuO-Fe_2O_3$ ferrite in this experiment could be expected to melt below the conventional sintering temperature of ferrite, ~ 1200 °C, and to locate preferentially at the grain boundary in the matrix of Ni–Zn ferrite, as shown in Fig. 5.

According to past investigations [5], non-uniform magnetic properties caused by compositional inhomogeneity of the sintered ferrite increase eddy current loss and, consequently, total loss of the ferrite. This resulted in an increase in the total loss, with which thinner matching thickness can be expected [1].

A Smith chart in Fig. 6 illustrates input impedance variation for sintered Ni–Zn ferrite without and with 5 wt % Composition C of the $CuO-Fe_2O_3$ system. Impedance values represented by the circumference in the Smith chart indicate 100% reflection and that by the centre point, 100% absorption. In reality, 99.0%

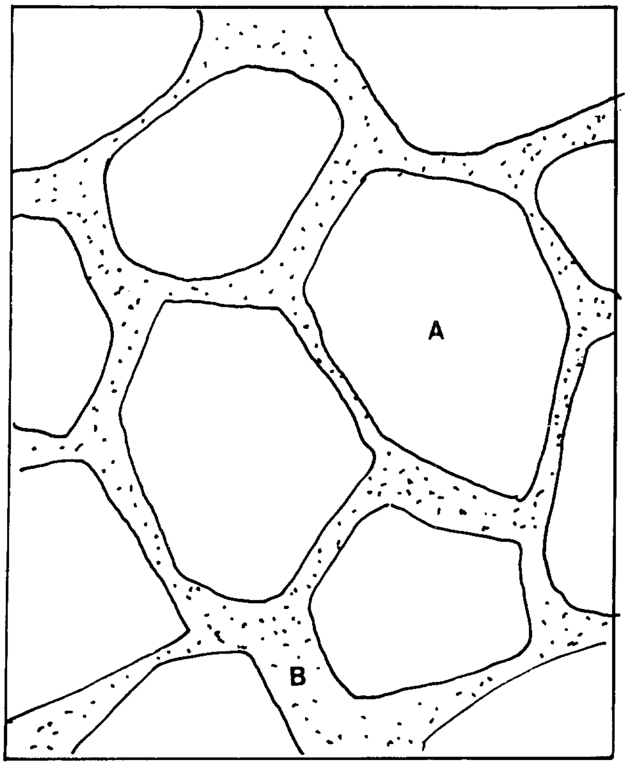

Figure 5 Schematic representation of the microstructure of sintered ferrite with $CuO–Fe_2O_3$ systems. A, Ni–Zn matrix system; B, $CuO–Fe_2O_3$ systems.

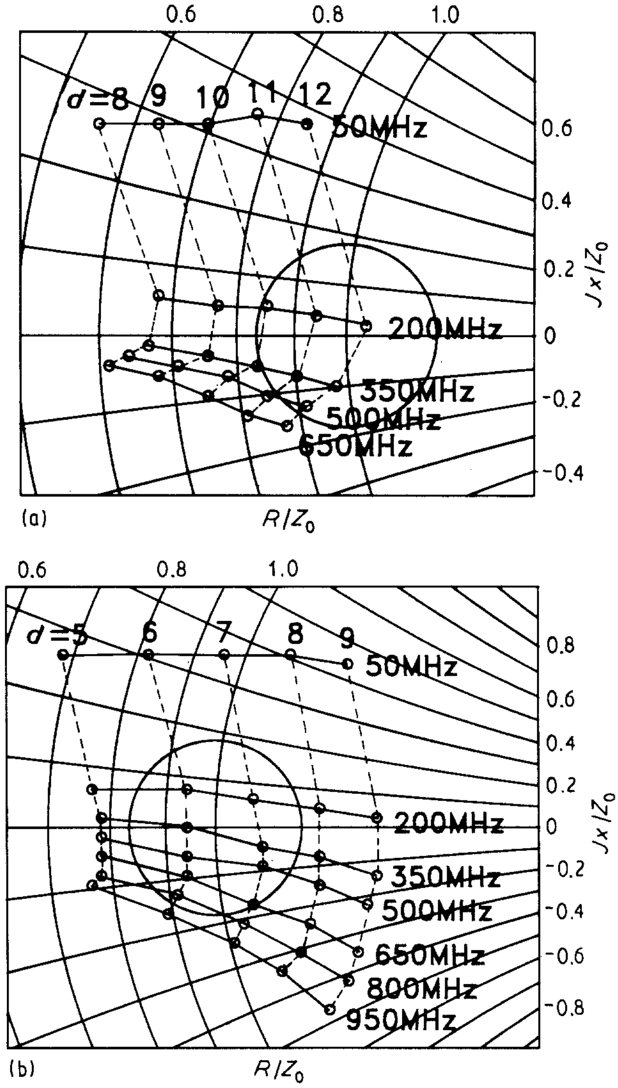

Figure 6 Loci of input impedance for (a) monolithic Ni–Zn ferrite, (b) Ni–Zn ferrite with 5 wt % $CuO–Fe_2O_3$ (Composition C) *d* is the thickness (mm).

absorption (1% reflection) is adopted as a practical limit for reflection conditions, because real electromagnetic waves to be absorbed spread broadly in frequency, and matching conditions vary with change in frequency. Matching ranges defined in this manner correspond to less than 1 of $(Z_{in(2)} - 1)/(Z_{in(2)} + 1)$ in the absolute value and the inside area of the small circle on the Smith chart.

Compared to monolithic ferrite, ferrites with Composition B of $CuO–Fe_2O_3$ were previously shown to exhibit a broader effective frequency range and decreased matching thickness. Magnetic loss in ferrite materials, divided into eddy current loss, residual loss by the resonance phenomenon and hysteresis loss by an external magnetic field, can be formulated as [8]

$$\begin{aligned} \tan\delta_m &= \tan\delta_h + \tan\delta_f + \tan\delta_r \\ &= k_1 B + k_2 f + k_3 \qquad (1) \end{aligned}$$

where k_1, k_2 and k_3 are constants, $\tan\delta_m$, $\tan\delta_h$, $\tan\delta_f$, $\tan\delta_r$, B and f represent total loss, hysteresis loss, eddy current loss, residual loss, flux density and frequency, respectively. When a ferrite is used as the wave absorber (no hysteresis loss), eddy current loss increases linearly with increasing frequency. On the other hand, residual loss maintains a constant value irrespective of frequency up to the resonance frequency, above which it abruptly increases and becomes a dominant loss source. This frequency-dependence of magnetic loss is schematically presented in Fig. 7. It should be noted that the eddy current loss contributes dominantly in the low-frequency range below the resonance frequency. This explains why $CuO–Fe_2O_3$ addition to ferrite exhibits a wave absorbing property in the low

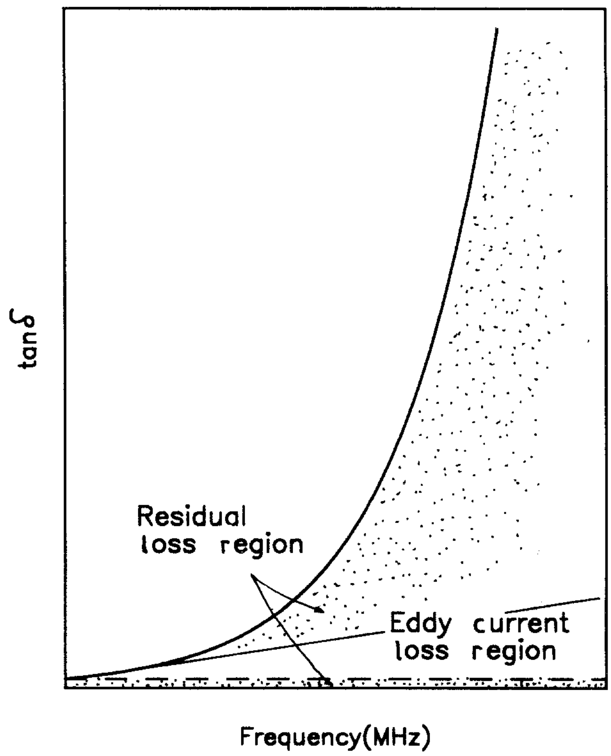

Figure 7 Schematic representation of $\tan\delta$ of the ferrite.

frequency range, where monolithic ferrites were ineffective.

The centre frequency (frequency at the maximum point of the attenuation curve) shift is presumed to occur because Ni–Zn ferrite with $CuO–Fe_2O_3$ behaves like a mixture of two ferrites with loss characteristics at the different frequency ranges. This effect occurs in all compositions of the $CuO–Fe_2O_3$ system, as shown in Table II. The more $CuO–Fe_2O_3$ is added, the higher the centre frequency moves to. This trend becomes clearer with increasing CuO/Fe_2O_3 ratio.

Scanning electron micrographs of sintered Ni–Zn ferrites with 1, 3 and 5 wt % Composition C $CuO–Fe_2O_3$ are compared with that of monolithic Ni–Zn ferrite in Fig. 8. $CuO–Fe_2O_3$ addition effectively enhanced the development of homogeneous

TABLE II Properties of sintered samples with the $CuO–Fe_2O_3$ system

CuO	Fe_2O_3	Amount of addition (wt %)	μ'' (50 MHz)	Thickness (mm)[a]	Frequency range (MHz)[b]
40	60	1	123	7.0	113–725
		3	115	7.3	130–800
		5	127	6.5	141–800
45	55	1	122	7.2	98–683
		3	128	6.7	98–800
		5	124	6.8	137–875
50	50	1	118	7.4	106–725
		3	120	7.2	122–875
		5	129	6.4	148–875
55	45	1	119	7.3	110–762
		3	126	6.7	143–800
		5	117	7.0	151–950
60	40	1	123	7.0	118–800
		3	125	6.8	125–821
		5	132	6.1	149–830
Monolithic Ni–Zn ferrite			65	11.7	139–530

[a] Matching thickness.
[b] Effective frequency range.

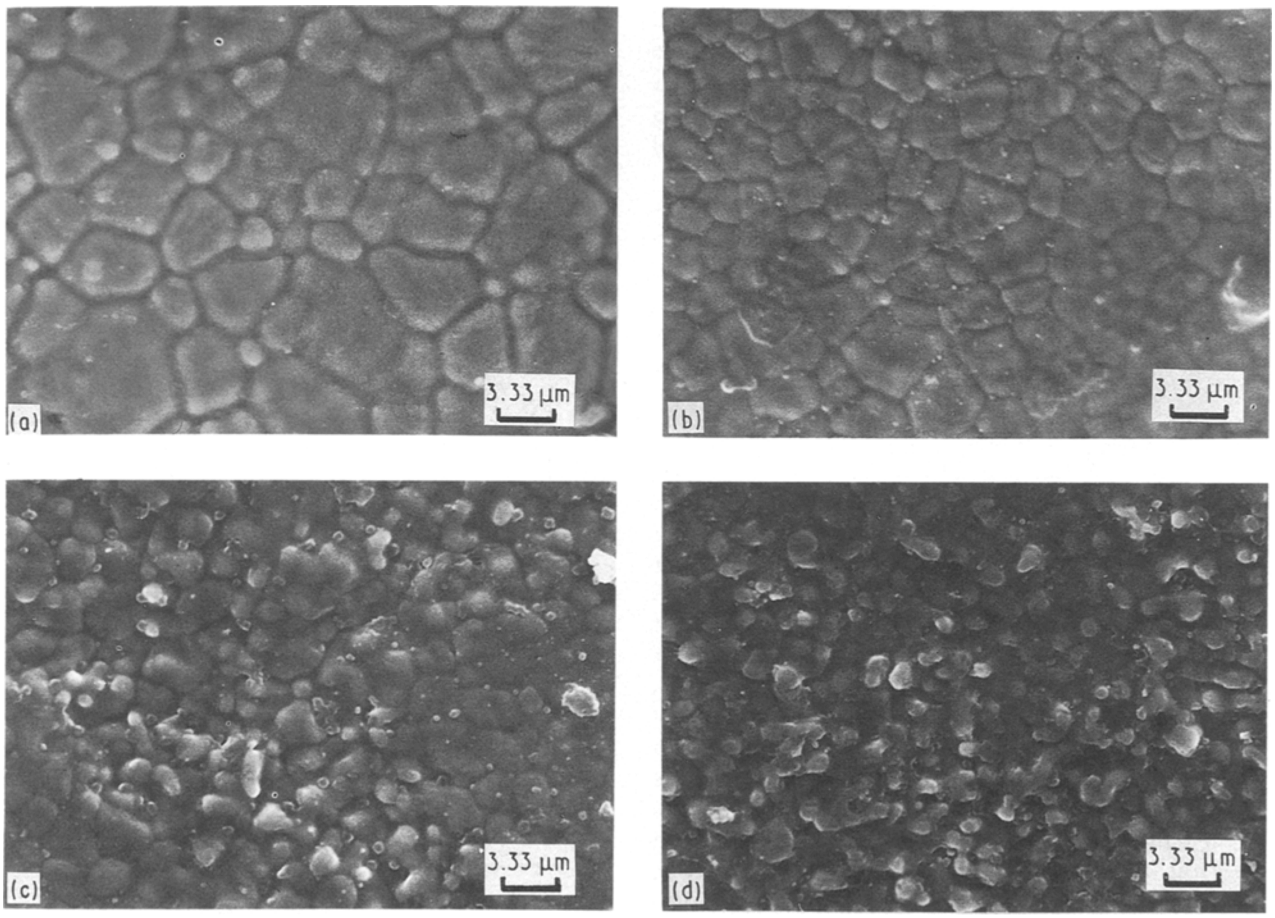

Figure 8 Scanning electron micrographs of sintered ferrite bodies. (a) Monolithic Ni–Zn ferrite. (b) 1 wt % addition of Composition C. (c) 3 wt % addition of Composition C. (d) 5 wt % addition of Composition C.

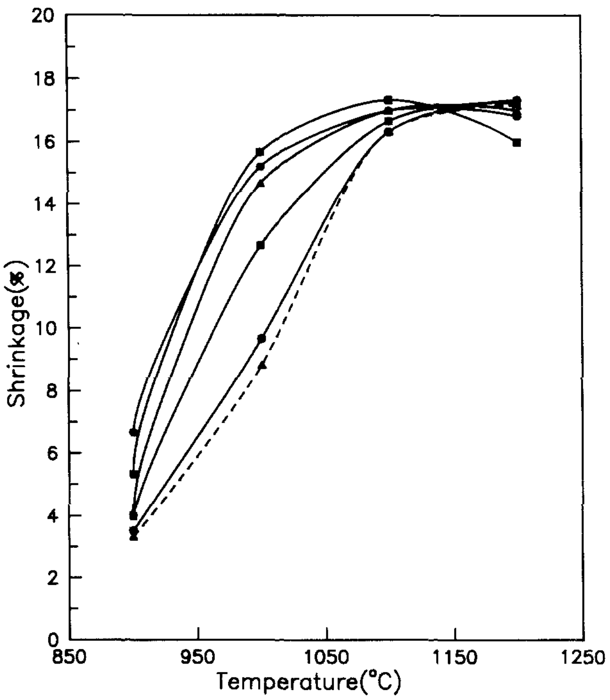

Figure 9 Shrinkage curves of sintered Ni–Zn ferrite with and without addition of 5 wt % of (○) A, (□) B, (△) C, (■) D and (●) E, and (▲) monolithic Ni–Zn.

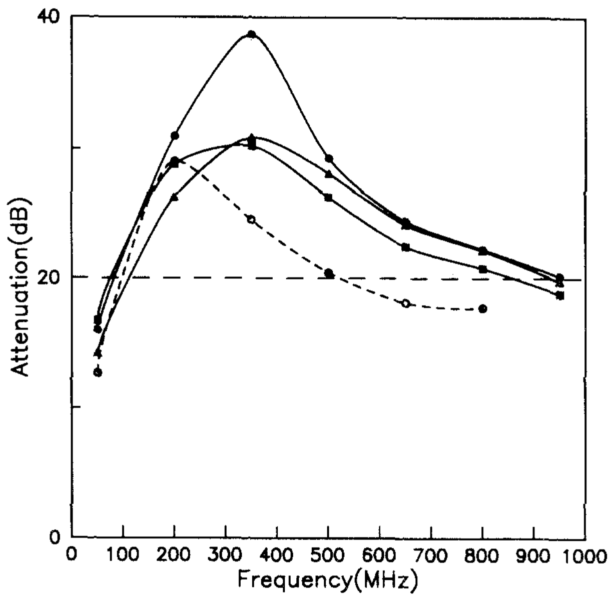

Figure 10 Attenuation behaviour against frequency of wave absorber with and without additives. Absorber thickness: (○) Monolithic ferrite, 11 mm; (■) 1 wt % Composition C 7 mm; (●) 3 wt % Composition C 7 mm; (▲) 5 wt % Composition C 6 mm.

microstructure with finer grain size. Fig. 9 shows the shrinkage curves of sintered Ni–Zn ferrite with and without 5 wt % $CuO–Fe_2O_3$ systems. Fig. 10 shows the attenuation behaviour of Ni–Zn ferrite with and without $CuO–Fe_2O_3$ systems: addition of $CuO–Fe_2O_3$ to Ni–Zn ferrite reduces the thickness and widens the effective frequency range of wave absorbers.

4. Conclusion

In this study, effects of $CuO–Fe_2O_3$ with ferritic crystal structure and magnetic property added to the ferrite matrix as liquid former, were investigated. The following conclusions were derived.

1. $CuO–Fe_2O_3$ system added to ferrite was found to be an effective liquid-forming sintering aid. With its addition, homogeneous and fine grain-size sintered ferrite could be obtained.

2. The $CuO–Fe_2O_3$ system exhibited common magnetic properties of spinel ferrites and possessed its own wave-absorbing property.

3. The addition of $CuO–Fe_2O_3$ to ferrite matrix moved the centre frequency of the wave absorber to high frequency, induced a decrease in matching thickness and increased the effective frequency range. These effects increased with increasing amount of $CuO–Fe_2O_3$ or the CuO/Fe_2O_3 ratio.

References

1. K. ISHINO, *Jpn. Electron. Ceram.* **19**(95) (1988) 20.
2. T. INUI "Electromagnetic Wave Absorber-Application of Ferrite By-product," NEC Technical Report, **37**(9) (1984) pp 2–13.
3. K. SUETAKE *et al.*, US Pat. 3754255, (1973).
4. FUJIDA IND., Jap. Pat. 2-16038, (1990).
5. K. ISHINO *et al.*, *Amer. Ceram. Bull.* **66** (1987) 1469.
6. A. M. NICOLSON *et al.*, *IEEE Trans. Instrum. Meas.* **IM-19** (1970) 377.
7. Y. NAITO and K. SUETAKE, *IEEE Trans. Micro. Theory Tech.* **MTT-19**(1) (1971) 65.
8. E. C. SNELLING, "Soft Ferrite–Properties and Application", 2nd Edn (Butterworth, 1988) pp. 33–9.

Received 1 May
and accepted 12 September 1991